Volume 13 Number 17 1985 Nucleic Acids Research

Site-specific nicking at the avian retrovirus LTR circle junction by the viral pp32 DNA endonuclease

Duane P.Grandgenett and Ajaykumar C.Vora

Institute for Molecular Virology, St.Louis University School of Medicine, 3681 Park Avenue, St.Louis, MO 63110, USA

Received 29 March 1985; Revised and Accepted 8 August 1985

ABSTRACT

The avian retrovirus pp32 DNA endonuclease prefers to nick supercoiled DNA containing long terminal repeat (LTR) circle junction sequences at one or the other of two sites, each which mapped two nucleotides back from the circle junction. The sequence at the sites of nicking was

C A↓ T T | A A T G,
G T A A | T T↑ A C

where ↑ indicates the positions of the two alternative nicked sites. This site-specific nicking was observed when the circle junction LTR DNA was present in supercoiled form, the divalent metal ion was Mg^{2+} and the molar ratio of protein to DNA was low. The majority of other LTR DNA sites nicked by pp32 in the presence of Mg^{2+} were adjacent to or within the dinucleotide CA.

INTRODUCTION

The avian retrovirus polymerase (pol) gene encodes a partially phosphorylated 32,000 dalton polypeptide (pp32) which possesses DNA nicking activity in the presence of Mg^{2+} or Mn^{2+} (1). Nicking of supercoiled DNA by the pp32 protein in the presence of Mg^{2+} results in the generation of unit-length and circular single-stranded (ss) DNA molecules as analyzed by alk aline sucrose gradient centrifugation (1). A Mn^{2+}-dependent DNA nicking activity is also associated with the parental molecule of pp32, the 92,000 dalton β polypeptide (2-4). The DNA polymerase of avian retroviruses exists in two forms, as a αβ or ββ dimer, both possessing Mn^{2+}-dependent DNA nicking activity (4). The 63,000 dalton α subunit in the αβ complex is derived from the NH_2 terminus of β (5) by proteolytic cleavage while the pp32 moiety is located at the COOH terminus of β (5,6,7). In addition, a small polypeptide possessing a molecular weight of 4,100 daltons is apparently encoded at the extreme 3'terminus of the pol gene and is not associated with either pp32 or β (8).

The Mn^{2+}-dependent DNA nicking activity of pp32 is approximately 10 - fold higher than that observed in the presence of Mg^{2+} (1). The DNA nicking

activity of αβ is virtually inactive when Mg^{2+} is substituted for Mn^{2+} (2-4) although partial chymotrypsin digestion of αβ in vitro results in the activation of Mg^{2+}-dependent nicking activity because of the release of the pp32 moiety from the β polypeptide (9). Both enzymes prefer supercoiled DNA as substrates. Alkaline sucrose gradient centrifugation analysis of ColE1 DNA which was nicked by pp32 and subsequently cleaved by EcoRI suggested that a limited number of preferred regions for pp32 nicking activity existed on this DNA; this apparent site-specificity was lost in the presence of Mn^{2+} (1).

The pp32 protein preferentially binds to specific regions on viral LTR DNA including the circle junction as demonstrated by using the nitrocellulose filter binding assays or DNase I-protection experiments (10,11). The termini of viral LTRs of integrated proviruses map 2 bp from the LTR circle junction found in unintegrated circular viral DNA (for review, see 12). The circular viral molecule containing two LTRs in tandem is the presumed precursor molecule to the integrated provirus (13,14). It has been shown that the Mn^{2+}-dependent DNA nicking activity associated with αβ DNA polymerase using (ss)DNA substrates selectively cleaved the plus or minus viral DNA strand at the LTR circle junction resulting in 6 bp staggered nicks (15). In this report, we examined the nicking of the LTR DNA circle junction region by pp32 in the presence of Mg^{2+} and Mn^{2+} using supercoiled and linear double strand(ds) DNA as substrates.

MATERIALS AND METHODS

The plasmid designated pPvuII-DG contained two complete copies of Schmidt-Ruppin LTR DNA in tandem (16). Supercoiled pPvuII-DG was nicked by pp32 in buffer containing 20 mM Tris·HCl(pH 7.5), 3 mM dithiothreitol (DTT), 50 mM NaCl, 0.1 mM EDTA and 3 mM $MgCl_2$ at various temperatures, times and protein concentrations as indicated in the figure legends. It should be emphasized that under these above assay conditions the pp32 protein can nick only one strand per supercoiled DNA molecule (1). Linear dsDNA was also subjected to αβ DNA polymerase or pp32 nicking in the same buffer except in the presence of 1 mM $MnCl_2$. Control DNA was treated identically as above except no enzymes were present. In all assays, the enzymes were preincubated with the DNA for 5 min at 25°C prior to initiation of the nicking reaction with divalent metal cation. The nicking reaction was stopped with 13 mM EDTA and by phenol extraction. Several labeling strategies were utilized to identify the location of nicks introduced by the enzymes near the circle junction between the tandem copies of LTR DNA. Usually, one-half of

the nicked DNA sample was digested with EcoRI and then SphI, followed by end-labeling of the minus viral DNA strand (bottom strand at R180, Fig. 3) by Klenow DNA polymerase in the presence of ^{32}P-α-dATP at 10°C for 25 min. To ensure complete fill in of the EcoRI site, unlabeled dATP and dTTP at a final concentration of 0.1 mM were added and the mixture was incubated for 15 additional min. The other half of the DNA sample was digested with EcoRI, dephosphorylated by bacterial alkaline phosphatase followed by end -labeling with ^{32}P-γ-ATP and T4 polynucleotide kinase. The labeled DNA was subsequently digested with SphI. This procedure resulted in end-labeling of the EcoRI site on the viral DNA plus strand. To isolate a DNA fragment labeled at the other LTR DNA EcoRI site (L180, Fig. 3), the labeled DNAs were digested with HinfI before isolation on polyacrylamide gels. With all of the above DNA modifying enzymes, minimal concentrations of enzymes were utilized to minimize contaminating nucleases thereby decreasing background problems. The above appropriate end-labeled DNA fragments were isolated on 5% polyacrylamide gels, electroeluted in a Tris-borate-EDTA buffer (45 mM Tris, pH 8.3; 45 mM boric acid,1 mM EDTA) and purified by DEAE-cellulose chromatography. After several ethanol precipitations, the samples were analyzed on 6% polyacrylamide DNA sequencing gels with the appropriate sequence markers (17). All cpm are expressed as Cerenkov cpm and the gels were exposed for the indicated number of days in the absence of an intensifying screen.

In addition to supercoiled plasmid as a DNA substrate, the same labeled pPvuII-DG DNA fragments described above containing the circle junction were isolated by polyacrylamide gel electrophoresis and purified by DEAE-cellulose chromatography. These linear DNA fragments were incubated with pp32 or αβ DNA polymerase under similar nicking conditions described above in the presence of Mn^{2+} or Mg^{2+}. After incubation, the reactions were stopped with 13 mM EDTA and 1 μg of yeast tRNA was added. Following phenol treatment and ether extraction, the samples were ethanol precipitated several times. The nicked DNA was analyzed on 6% polyacryamide DNA sequencing gels with the appropriate sequence markers.

The AMV pp32 protein was purified through poly(U)-Sepharose chromatography and in some experiments through an additional glycerol gradient sedimentation step (11). The AMV αβ DNA polymerase was purified through Heparin-Sepharose 4B chromatography (2). Both proteins were purified to near homogeneity.

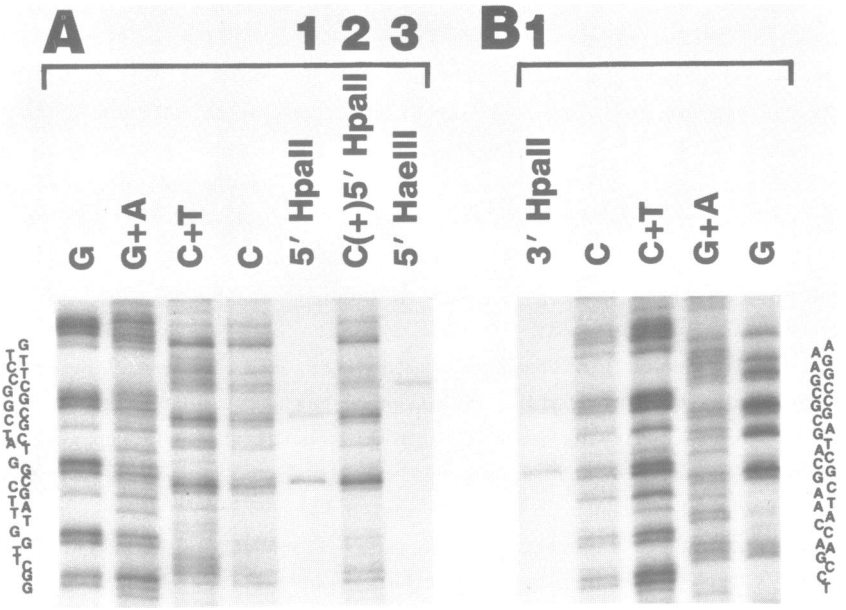

Figure 1: Comparison of electrophoretic mobilities of sequence ladders and aligned restriction fragments containing two HpaII sites and one HaeIII site cleaved by the corresponding enzymes. A. The EcoRI/SphI fragment of pBR322 was 5' end-labeled at the EcoRI site and was subsequently cleaved with HpaII (lane 1, 400 cpm); lane 2, chemical C reaction plus cleaved HpaII fragment (400 cpm); lane 3, HaeIII restriction of above fragment (200 cpm). The autoradiograph also shows Maxam and Gilbert (17) sequence ladders of the EcoRI/SphI fragment. The DNA sequencing gel was exposed for 5 days. B. The same EcoRI/SphI fragment of pBR322 was 3' end-labeled at the EcoRI site and was subsequently cleaved with HpaII (lane 1, 270 cpm). The sequence markers are shown for the EcoRI/SphI fragment. The gel was exposed for 1 week.

RESULTS

Defining parameters for the DNA nicking assays

We wanted to determine the specificity of pp32 nicking on linear dsDNA which contained the circle junction of avian retrovirus LTR DNA. To increase the sensitivity and specificity of the DNA nicking assay, we used 5' and 3' end-labeled restriction fragments. By comparison of the electrophoretic mobilities of Maxam and Gilbert (17) sequence ladders to the length of the end-labeled denatured fragment, the exact location of the nick in the DNA could be identified. To ensure that the assay was correct, we digested 5' or 3' end-labeled control DNA fragments at specific locations with restriction enzymes. The 5' end-labeled EcoRI/SphI fragment (565 bp in length)

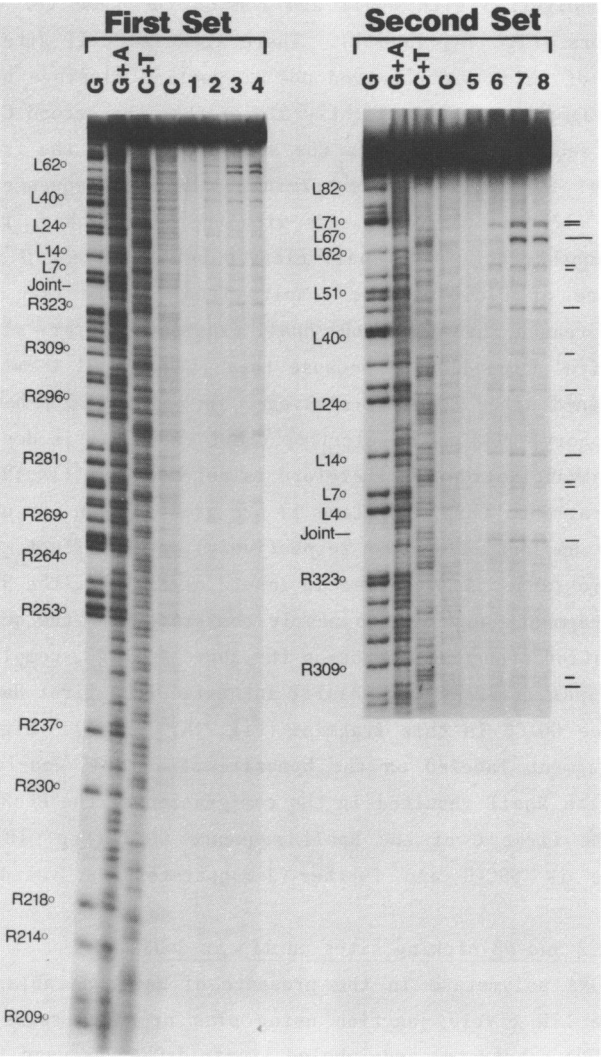

Figure 2: Mapping of pp32 and αβ DNA polymerase nicked sites on plus strand LTR DNA using a linear dsDNA substrate. Approximately 0.02 μg of 5' end-labeled 248 bp DNA fragment (82 Kcpm) was incubated with standard reaction buffer in the presence or absence of enzyme at 37°C with 1 mM $MnCl_2$ present. The reactions were stopped at various times and the DNA was examined on a DNA sequencing gel. (First Set). Lane 1, Control DNA for 20 min; lane 2, 1.2 μg of pp32 for 10 min; lane 3, 0.38 μg of αβ for 15 min; lane 4, 0.38 μg of αβ for 25 min. The first set of samples and markers were run for 110 min. Exposure of the film was for 1 week. (Second Set). Lanes 5 to 8 are in the same order as lanes 1 to 4 as described above except the samples were run for 260 min under the same electrophoresis conditions. The gel was exposed for 4 days. The horizonal lines on the right side of the gel correspond to the nicked sites.

of pBR322 was digested with HpaII and run on the same gel with chemical sequence markers (Fig. 1A, lane 1). There are six HpaII sites in this DNA fragment, two of which are observed due to partial cleavage by HpaII. The EcoRI/HpaII fragments migrate slightly slower than the second C in the HpaII recognization sequences, CCGG. In the sequence ladder, the fragment representing C (Fig. 1A) has lost this terminal C as a consequence of the chemical cleavage (17) and therefore ends with the 5' neighbor, in this particular case, another C. Thus, HpaII cleaves between C and C in the recognition sequence of C↓CGG. These results thus confirm that our assay is correct. The reason that the EcoRI/HpaII fragments migrate slightly slower than the chemical C product is because they lack the 3' terminal phosphate which is retained after chemical cleavage. The effect of removing a single terminal phorphoryl residue on electrophoretic mobility is dependent on the size of the polynucleotide and therefore is not constant (18,19). Since the EcoRI/HpaII fragments (Fig. 1A, lane 1) are greater than 100 nucleotides in length, (161 bp and 170 bp, respectively), the effect of phosphate approaches zero (18). As observed in lane 2 of Fig. 1A, the 5' end-labeled EcoRI/HpaII fragments appeared to nearly comigrate with the second C of the CCGG recognization sequence. By using the above analogy, complete digestion of the EcoRI/SphI fragment with HaeIII identified the first HaeIII recognization sequence GG↓CC in this fragment (Fig. 1A, lane 3). Digestion of the EcoRI/SphI fragment labeled on the opposite strand (3' end-labeled at the EcoRI site) with HpaII resulted in the comigration of the EcoRI/HpaII fragments with the first C of the HpaII sequence GGCC (Fig. 1B). Thus, the cleavage site is GGC↓C and further demonstrates the validity of these assays.

Mapping of pp32 and αβ nicking sites on linear dsDNA

The αβ DNA polymerase in the presence of Mn^{2+} was able to nick 3 bp back from the LTR circle junction using plus or minus ssDNA. Instead of using this ssDNA substrate, end-labeled linear dsDNA was used for comparison of αβ DNA polymerase and pp32 nicking properties. The 248 bp EcoRI/SphI DNA fragment containing the LTR circle junction (See Fig. 3 and 8) and 5' end-labeled on the viral plus strand, was incubated with pp32 or αβ in the presence of 1 mM $MnCl_2$ at 37°C (Fig. 2). In the first set of experiments with control DNA, no major nicked fragments were observed indicating that at this level of Mn^{2+}, nonspecific breakage of DNA is not occurring (Fig. 2, lane 1) (10). Incubation of the 248 bp fragment with pp32 resulted in a variety of nicked fragments with the majority of the nicked sites located to the right of the circle junction (Fig. 2, lane 2 and Fig. 3). The αβ DNA

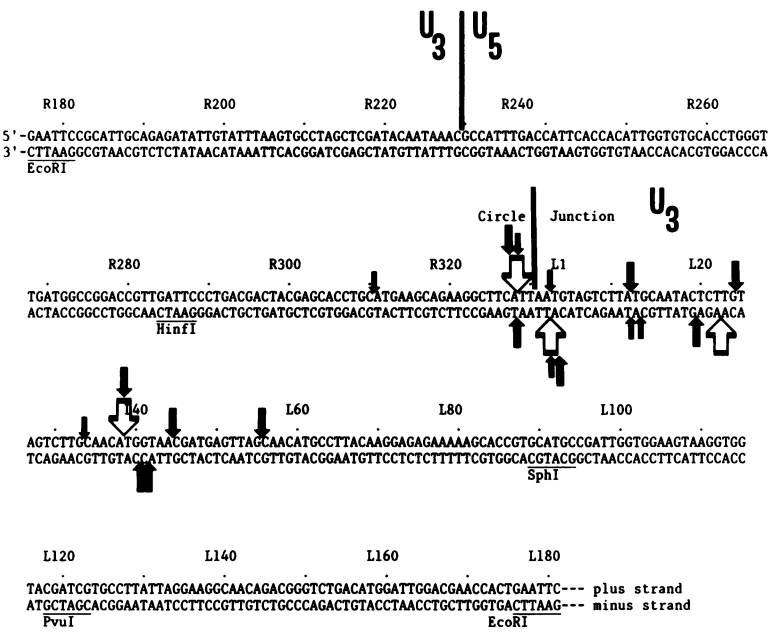

Figure 3: Map positions of pp32 nicking sites on a supercoiled LTR DNA substrate. The plus and minus viral LTR DNA sequences which are located on either side of the circle junction (designated as joint on figures) are shown (top and bottom, respectively). The height of the arrows roughly represent the nicking frequency occurring within the strand per inspection of band intensities of exposed x-ray film. The open arrows located on the top and bottom sides of the LTR sequence represent the major nicks introduced into supercoiled DNA by pp32 in the presence of Mg^{2+}; the closed arrows represent nicks generated by pp32 in the presence of Mn^{2+} (Fig. 4, 5 and 6). The R lettered numbers refer to the terminal repeat sequences adjacent to the src region on the right end of the linear map of unintegrated viral DNA, whereas the L lettered numbers refer to terminal repeat adjacent to the gag region on the left end of the linear map. The terminal repeats (partially shown) consists of two identical copies (330 bp in length), each of which contains the region unique to the 3' terminus (U3) and the 5' terminus (U5) of the viral genome. The EcoRI, HinfI, SphI and PvuI restriction sites are shown.

polymerase also nicked the 248 bp fragment generating essentially the same species as pp32 (Fig. 2, lanes 3 and 4) except for two nicked fragments at the top of the gel between L62 and L71 (see below).

In the second set of experiments in Fig. 2, the same DNA samples were run for a longer time permitting detailed mapping of the nicked fragments. Again, there is no outstanding differences in the DNA nicking patterns observed between αβ and pp32 using linear DNA (Fig. 2) or supercoiled DNA (see below) suggesting similar nuclease mechanisms for these enzymes in the

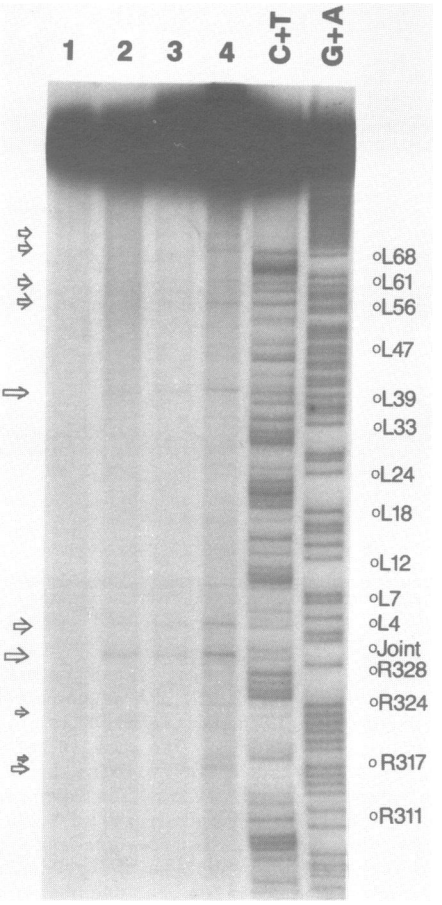

Figure 4: Mapping the location of nicks introduced by pp32 on the plus strand of viral LTR DNA using supercoiled DNA as substrate. pPvuII-DG (3 μg) was incubated in the presence or absence of pp32 at 37°C for 1 h under standard assay conditions with 3 mM $MgCl_2$. The reactions were stopped, phenol extracted, digested with EcoRI and the DNA was 5' end-labeled at the EcoRI site as described in Materials and Methods. The labeled DNA was digested with SphI and the labeled 248 bp fragment was isolated. Lane 1, Control DNA, 22,000 cpm; lane 2, 1.06 μg of pp32, 22,000 cpm; lane 3, 2.12 μg of pp32, 25,000 cpm; lane 4, same as lane 3 except 48,000 cpm; markers C+T and G+A. The gel was exposed for 10 days.

presence of Mn^{2+}. This same relative pattern of nicking by pp32 or αβ in the presence of Mn^{2+} was observed under a variety of conditions including a 4-fold range in protein concentration, incubation at 25°C and at slightly higher or lower NaCl concentrations (data not shown). The molar ratio of enzyme to linear DNA varied between 75 to 1 and 300 to 1, respectively. As

reported previously (10), pp32 or αβ DNA polymerase in the presence of Mg^{2+} were not able to nick the 248 bp fragment.

The same 248 bp EcoRI/SphI DNA fragment labeled on the minus viral strand was incubated in the presence of either αβ or pp32 (data not shown). Again, the pattern of nicked fragments with either enzyme were nearly identical, even at substantially lower αβ protein concentration then used previously (Fig. 2).

The above experiments permit several conclusions. First, the αβ DNA polymerase and the pp32 protein active endonuclease sites appear to recognize the same nucleotide sequences in the presence of Mn^{2+}, although slight differences are apparent. There is no obvious overall nucleotide consensus sequence but many of the sites have two adjacent cleavage events demonstrating that the enzymes recognize these particular sites more frequently than most single cleavage events. Slightly over half of the nicked sites are adjacent to or within the dinucleotide CA (data not shown) suggesting that these dinucleotides are recognized preferentially over other sets of dinucleotides (see below also). Finally, as previously observed with αβ using ssDNA as substrate (15), 6 bp staggered nicks are generated at the circle junction but are not a major population under these conditions using linear dsDNA.

Increased specificity of pp32 nicking of LTR DNA under the constrain of DNA superhelicity.

The pp32 protein prefers supercoiled DNA both for nicking (1) and binding substrates (11). Mapping the location of the nicked sites (Fig. 3) generated by pp32 on the plus strand DNA around the circle junction using supercoiled pPvuII-DG as substrate and Mg^{2+} as divalent metal ion revealed an interesting result. The nucleotide sequence of the pPvuII-DG clone was previously determined (16). The major labeled DNA fragment (Fig. 4, lane 2, 3 & 4) generated by pp32 nearly comigrated with the "T" sequence marker (R329). As stated above, this slower migration of the cleaved fragment is due to the absence of a terminal phosphate. Thus, pp32 nicks at the sequence CA↓TT. The open arrows in figure 3 identify the major nicked sites generated by pp32 using supercoiled DNA as substrate. These data demonstrate that pp32 is capable of mimicking the *in vivo* observation that 2 bp are removed from the terminus of the LTR DNA by a 4 bp staggered nick at the circle junction upon integration of viral DNA (12). However, it is also very apparent that pp32 is capable of introducing a variety of nicks at various locations under these assay conditions (Fig. 4, lanes 2 to 4). The nicked sites are at R315, R316, R322, R328, L2, L38, L55, L60, L67 and L73.

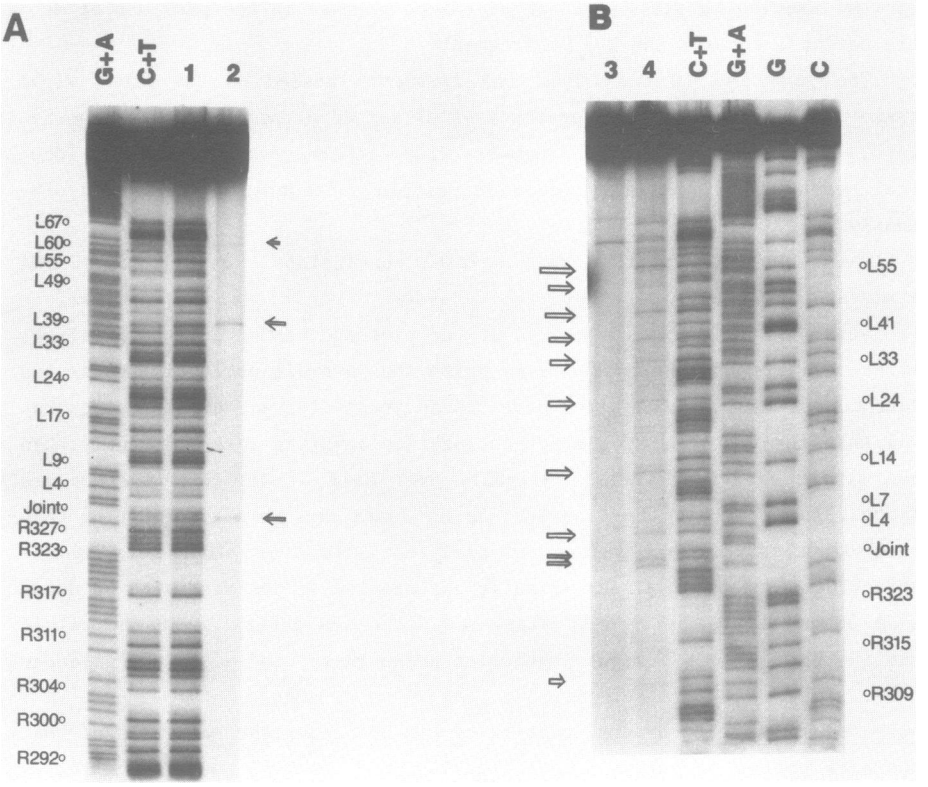

Figure 5: Comigration of pp32 generated LTR DNA fragment with "T" chemical sequence marker and nicking of pPvuII-DG by pp32 with Mn^{2+}. A. Supercoiled pPvuII-DG DNA (3 µg) was incubated with pp32 (1.2 µg) at 37°C for 30 min under standard assay conditions with 3 mM $MgCl_2$. The plus strand DNA fragment was labeled and isolated as described in Fig. 4. Markers G+A and C+T. Lane 1, C+T markers plus 50,000 cpm of pp32 nicked fragment; lane 2, 43,000 cpm of pp32 nicked fragment only. The gel was exposed for 4 days. B. Supercoiled pPvuII-DG(1.5 µg) was incubated with pp32 at 37° for 5 min with 1 mM $MnCl_2$. The plus strand DNA fragment was labeled as above. Lane 3, control DNA 74,000 cpm; lane 4, 0.53 µg of pp32, 76,000 cpm. Markers C+T, G+A, G and C. The gel was exposed for 5 days.

Again, a majority (60%) of the nicked sites are adjacent to or within the dinucleotide CA.

Assay conditions were varied to increase the specificity of the nicked sites generated by pp32. The specificity of this reaction was increased by merely decreasing the incubation time at 37°C to 30 min (Fig. 5A, lane 2) instead of 1 hr (Fig. 4) with a protein to DNA ratio of 40 to 1. The conversion of supercoiled to nicked circles was approximately 5%, comparable to

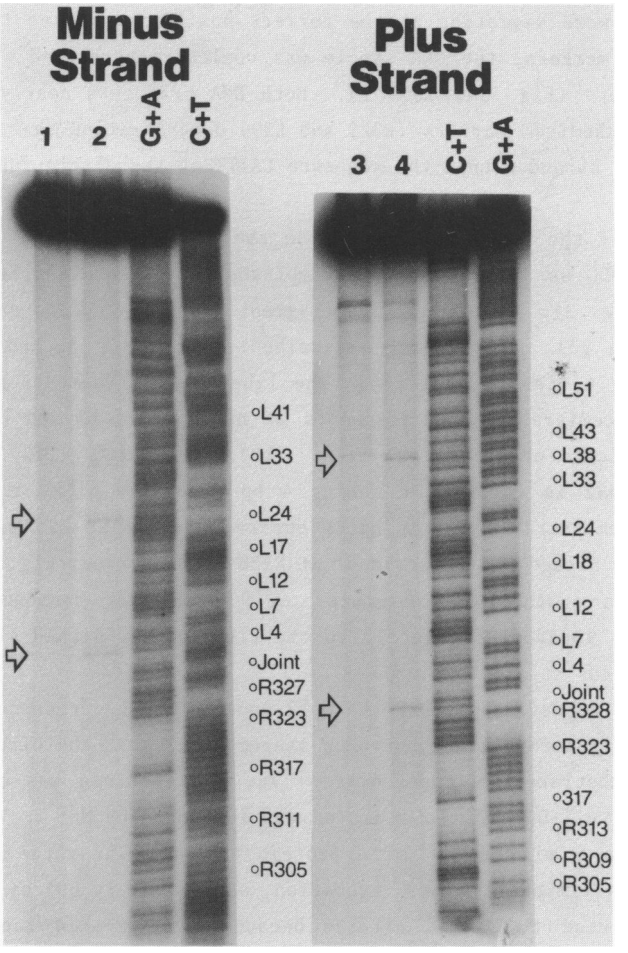

Figure 6: Mapping the location of nicks introduced by pp32 on the minus or plus strand of viral LTR DNA using supercoiled DNA as substrate. Minus-strand. pPvuII-DG (4.5 μg) was incubated in the presence (1.6 μg) and absence of pp32 at 37°C for 45 min under standard assay conditions with 3 mM $MgCl_2$. The reactions were stopped with EDTA, phenol extracted, digested with EcoRI and SphI and the DNA was 3' end-labeled on the minus strand at R180. The 248 bp fragment was isolated. Lane 1, 61,000 cpm of control DNA; lane 2, nicked DNA, 62,500 cpm. Plus strand. Aliquots of the above samples were also 5' end-labeled on the plus strand. The labeled DNA was digested with SphI and the labeled 248 bp fragment was analyzed. Lane 3, control DNA, 39,500 cpm; lane 4, 31,000 cpm of nicked DNA sample. The gel was exposed for 8 days.

previously published information (1). As is clearly evident in Fig. 5A (lane 2), only two major nicked species (R328 and L38) are observed, both containing the nicked sequence of CA↓T. To ensure that the pp32 generated

DNA fragments were migrating at the correct position relative to the chemical sequence markers, the DNA sample was coelectrophoresized with the C+T chemical markers (Fig. 5A, lane 1). Both DNA fragments nearly comigrated with the "T" chemical markers (R329 and L39) demonstrating that pp32 nicked the plus viral strand within the sequence CA↓TT at the circle junction (Fig. 3).

Mapping of the pp32 nicked sites on the LTR minus strand using supercoiled pPvuII-DG as substrate was accomplished by 3' end-labeling the EcoRI site (R180, Fig. 3). The 248 bp DNA fragment was isolated and analyzed on a DNA sequencing gel as previously described. Two major nicked sites were observed (Fig. 6, lane 2; Fig. 3). The labeled DNA fragments generated by pp32 nicking comigrated with fragments at nucleotides L3 and L23. Therefore, the nicks occurred at TT↓AC (L2) and GA↓AC (L22) (Fig. 3). Apparently, pp32 is capable of making 4 bp staggered nicks at the circle junction as demonstrated by the nicks observed either at L2 (minus strand, Fig. 6) on one nicked DNA molecule or at R328 (plus strand, Fig. 5A and Fig. 6, lane 4) on another DNA molecule. A 9 nucleotide consensus sequence (ACATCAGAA) is located immediately to the right of the nicked sites (L3 and L23) on the minus strand (Fig. 3).

We wanted to define whether the pp32 protein in the presence of Mn^{2+} (1 mM) could also generate a 4 bp or 6 bp staggered nick at the circle junction if the DNA substrate was supercoiled. The pp32 protein was complexed to supercoiled pPvuII-DG and the reaction was initiated by Mn^{2+}. The reaction was limited to 5 min at 37° at a protein to DNA molar ratio of 40 to 1. Even with this limited time of incubation, approximately 50% of supercoiled DNA was converted to nicked circles because Mn^{2+} greatly increases pp32 nicking capabilities (1). Figure 5B (lanes 3 and 4) clearly shows that under these nicking conditions, pp32 is capable of generating nicks at both 2 and 3 bp from the circle junction on the plus strand (Fig. 3, closed arrows). Thus, pp32 nicks within the sequence C↓A↓TT at the circle junction when Mn^{2+} is used. Similar results were obtained on the minus strand when pp32 nicked supercoiled pPvuII-DG with 1 mM $MnCl_2$ present (data not shown). In this case, the enzyme generated nicks 2 and 3 bp from the circle junction as illustrated (TT↓A↓C) (Fig. 3). These data demonstrate that pp32 in the presence of Mg^{2+} is capable of generating 4 bp staggered nicks at the circle junction but generates 4 and 6 bp staggered nicks on different DNA molecules in the presence of Mn^{2+}.

Further evaluation of the above data in Fig. 5B also shows that pp32

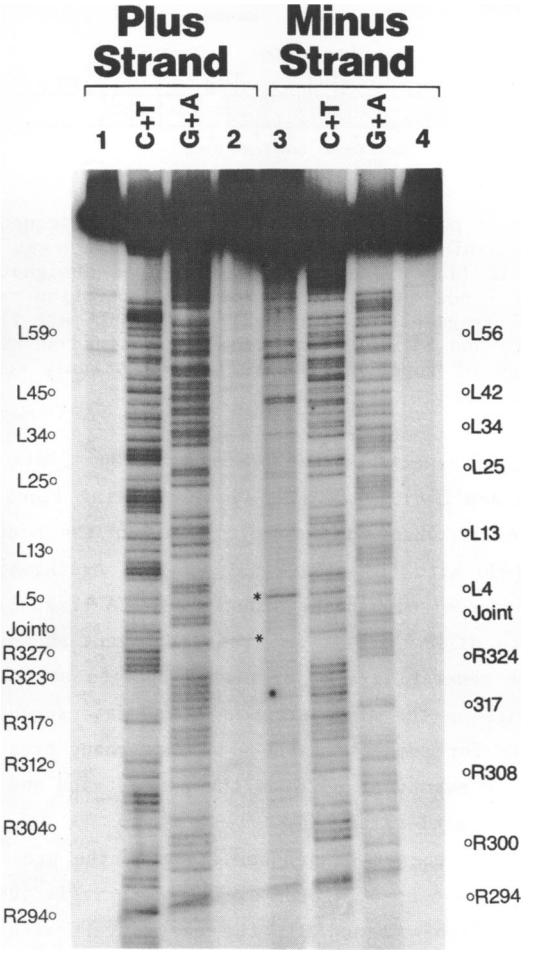

Figure 7: Mapping the location of nicks introduced by αβ DNA polymerase on the minus or plus strand of LTR DNA using supercoiled DNA as substrate. pPvuII-DG (1.5 μg) was incubated in the presence (1.9 μg) or absence of αβ under standard assay conditions with 1 mM $MnCl_2$ for 5 min at 37° C. Approximately 25% of the supercoiled DNA was converted to nicked circles. The reactions were stopped and the DNA was digested with EcoRI and SphI for labeling of the minus strand or EcoRI for labeling the plus strand as previously described. Plus Strand: lane 1, control DNA, 197,000 cpm; C+T and G+A chemical markers; lane 2, 180,000 cpm, αβ DNA polymerase. Minus Strand: lane 3, 44,000 cpm, αβ DNA polymerase; lane 4, control DNA 46,000 cpm; C+T and G+A chemical markers. The 6 bp staggered cut is marked by * in lanes 2 and 3 at the circle junction.

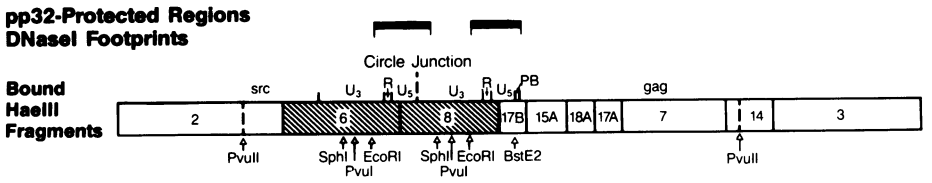

Figure 8: Summary of pp32 binding sites on viral LTR sequences. A 1670 bp viral fragment containing two tandam copies of LTR DNA was inserted at the PvuII site of pBR322 (16). The top two dark lines designate the region of LTR DNA which pp32 binds as analyzed by DNaseI protection experiments (10). Some of the HaeIII fragments generated from pPvuII-DG are illustrated. The shaded fragments (6 and 8) are preferentially retained on nitrocellulose by pp32 upon digestion of supercoiled pPvuII-DG previously complexed to pp32 (11).

generated 11 nicked fragments in the presence of Mn^{2+}, six of which (R328, L2, L12, L24, L33 and L44), were also observed using linear dsDNA (Fig. 2 and Fig. 3). Similar observations were made on the minus strand using supercoiled pPvuII-DG with Mn^{2+} (data not shown). Again, 50% of the nicked sites were adjacent to or within the dinucleotide CA (Fig. 3). Interestingly, in the presence of Mn^{2+} (Fig. 2, 3, 5B, data not shown), the pp32 protein is capable of generating a major nicked species at position L2 on the plus strand and R328 on the minus strand. These data suggest that pp32 may also be responsible for removal of the 4 bp 5'overhang presumably generated by the first nicking events at R328 on the plus strand and L2 on the minus strand upon integration of viral DNA.

We confirmed that the αβ DNA endonuclease in the presence of Mn^{2+} was capable of generating a 6 bp staggered nick at the circle junction (15). As observed in Fig. 7 (lanes 2 and 3), the enzyme generated major nicks at positions R327 (plus strand) and L3 (minus strand). Of the 18 nicked sites generated on either strand of supercoiled PvuII-DG by pp32 in the presence of Mn^{2+} (Fig. 3 and Fig. 5B), 10 sites were in common with those generated by αβ DNA endonuclease (data not shown).

DISCUSSION

We had previously failed to detect any major nicked sites generated by pp32 on a variety of supercoiled or linear dsDNA molecules using other less sensitive assay methods (11). However, it is apparent that both pp32 or αβ DNA polymerase under most assay conditions appear to nick DNA at a variety of sites. The observation that the αβ DNA polymerase was able to generate 6 bp staggered nicks at the circle junction of LTR DNA (15) prompted us to

determine if pp32, using a more sensitive assay procedure, was able to recognize the circle junction sequences. The pp32 protein was able to generate 4 bp staggered nicks at the circle junction, thus mimicking the in vivo observation that the 4 intervening bp are lost during integration of viral DNA (12). The apparent requirements for the preferential 4 bp staggered nick at the circle junction in vitro are that the DNA substrate be supercoiled and a relatively low protein to DNA ratio be maintained. Whether pp32 or αβ (15) endonuclease, both capable of generating 6 bp staggered nicks, are responsible for generating 6 bp staggered nicks on host cell DNA at the viral insertion site (12) is unknown.

The biological role(s) of the pp32 protein or the pp32 moiety located at the COOH terminus of β in the life cycle of retroviruses is still unknown. However, it is likely that this protein is involved in integration of viral DNA. It has recently been demonstrated genetically in the murine leukemia retrovirus that the 40,000 dalton DNA endonuclease (the counterpart of the avian endonuclease), is required for integration of viral DNA (20,21). Similar genetic data also exists with the spleen necrosis virus for the 3' terminus of the pol gene being involved in integration of viral DNA (22). In contrast, several avian virus mutants whose single base change occurred near the NH_2 terminus of the pp32 protein seemingly integrate viral DNA at near wild type levels (7,23). These mutants appear to replicate poorly and have decreased transforming ability relative to wild type RSV. Possibly, the pp32 protein and the pp32 moiety of β, or both, are multifunctional.

There is reasonable correlation between the various data obtained by comparing the interactions of pp32 with LTR DNA using the DNase I footprinting technique (10), the nitrocellulose filter binding assay (10,11) and the technique employed in this paper, DNA nicking assays. These data are summarized in Fig. 3 and Fig. 8. The pp32 protein, as analyzed by DNaseI protection experiments, forms a unique nucleosome-like structure on LTR DNA which encompasses the viral promoter in U_3, extends through U_5, and proceeds past the circle junction into U_3 for about 30 bp (see Fig. 8). Although it is likely that pp32 preferentially binds to the circle junction region, the protein can bind to and nick a variety of DNAs. Other highly specific DNA binding proteins likewise can bind to DNA at random locations in addition to unique sequences which are biologically important (see 10,11,24-27). Other factors including DNA-protein constraints occurring in vivo and involvement of either viral or cellular proteins in the integration process could signi-

ficantly alter pp32 binding and nicking of LTR DNA at the circle junction. One other possible viral protein involved in this process could be the 4,100 dalton polypeptide apparently encoded at the extreme 3' terminus of the avian retrovirus pol gene (8).

Although pp32 can nick DNA at a variety of sites particularly in the presence of Mn^{2+} (Fig. 3), the enzyme appears to nick DNA adjacent to or within the dinucleotide CA at a considerably higher frequency than other sets of dinucleotides. This observation is most apparent with Mg^{2+} as the divalent metal ion. Most proviruses terminate in host DNA with the sequences TG and CA as illustrated, cell DNA-TG-viral DNA-CA-Cell DNA (12). Interestingly, these same sets of dinucleotides are located at the termini of transposable elements structurally related to retroviruses (12). Since almost all eucaryotic transpositions end in CA, a nick must be made here to permit transposition (28). An understanding of the enzymatic mechanisms involved in recognization of CA dinucleotides by pp32 may contribute to our knowledge of the numerous DNA eucaryotic recombination events which occur at the CA dinucleotide sequence (28). The 3' terminal domain of RSV pol which encompasses the pp32 protein is conserved among various types of retroviruses (29) as well as the Drosophilia copia reverse transcriptase-like enzyme (30).

Acknowledgements

We thank Joseph Hoffman and Tapan Misra for their discussions. This work was supported by National Institute of Health Public Service Research Grant CA-16312. Thanks are also extended to Norma C. Urani for typing this manuscript.

REFERENCES

1. Grandgenett, D.P., Vora, A.C. and Schiff, D.P. (1978) Virology 89, 119-132.
2. Golomb, M. and Grandgenett, D.P. (1979) J. Biol. Chem. 254, 1606-1613.
3. Samuel, K.P., Papas, T.S. and Chirikjian, J.C. (1979) Proc. Natl. Acad. Sci. U.S.A. 76, 2659-2663.
4. Leis, J., Duyk, G., Johnson, S., Longiaru, M. and Skalka, A. (1983) J. Virol. 45, 727-739.
5. Copeland, T.D., Grandgenett, D.P. and Oroszlan, S. (1980) J. Virol. 36, 115-119.
6. Eisenman, R.N., Mason, W.S. and Linial, M. (1980) J. Virol. 36, 62-78.
7. Hippenmeyer, P.J. and Grandgenett, D.P. (1984) Virology 137, 358-370.
8. Grandgenett, D.P., Quinn, T., Hippenmeyer, P.J. and Oroszlan, S. (1985) J. Biol. Chem. 260, 8243-8349.
9. Grandgenett, D.P., Golomb, M. and Vora, A.C. (1980) J. Virol. 33, 264-271.

10. Misra, T.K., Grandgenett, D.P. and Parsons, J.T. (1982) J. Virol. 44, 330-343.
11. Knaus, R.J., Hippenmeyer, P.J., Misra, T.K., Grandgenett, D.P., Muller, V.R. and Fitch, W.M. (1984) Biochem. 23, 350-359.
12. Varmus, H.E. (1983) Retroviruses In "Mobile Genetic Elements" (J.A. Shapiro, ed.), pp. 411-503. Academic Press, New York.
13. Panganiban, A.T. and Temin, H.M. (1983) Nature 306, 155-160.
14. Panganiban, A.T. and Temin, H.M. (1984) Cell 36, 673-679.
15. Duyk, G., Leis, J., Longiaru, M. and Skalka, A.M. (1983) Proc. Natl. Acad. Sci. U.S.A. 80, 6745-6749.
16. Swanstrom, R., DeLorbe, W.J., Bishop, J.M. and Varmus, H.E. (1981) Proc. Natl. Acad. Sci. U.S.A. 78, 124-128.
17. Maxam, A.M. and Gilbert, W. (1980) Methods of Enzymology 65, 499-560.
18. Tapper, D.P. and Clayton, D.A. (1981) Nucl. Acid Res. 9, 6787-6794.
19. Schmid, K., Thomm, M., Laminet, A., Laue, G.G., Kessler, C., Stetler, K.O. and Schmitt, R. (1984) Nucl. Acid Res. 12, 2619-2628.
20. Schwartzberg, P., Colicelli, J. and Goff, S.P. (1984) Cell 37, 1043-1052.
21. Donehower, L.A. and Varmus, H.E. (1984) Proc. Natl. Acad. Sci. U.S.A. 81, 6461-6465.
22. Panganiban, A.T. and Temin, H. (1984) Proc. Natl. Sci. U.S.A. 81, 7885-7889.
23. Hippenmeyer, P.J. and Grandgenett, D.P. (1985) J. Biol. Chem. 260, 8250-8256.
24. Better, M., Lu, C., Williams, R.C. and Echols, W. (1982) Proc. Natl. Acad. Sci. U.S.A. 79, 5837-5841.
25. Payvar, F., DeFranco, D., Firestone, G.L., Edgar, B., Wrange, O., Okret, S., Gustafsson, J.A. and Yamamoto, K.R. (1983) Cell 35, 381-392.
26. Klevan, L. and Wang, J.C. (1980) Biochem. 19, 5229-5234.
27. Craig, N.L. and Nash, H.A. (1984) Cell 39, 707-716.
28. Rogers, J. (1983) Nature 305, 101-102.
29. Chin, I.M., Callahan, R., Tronick, S.R., Schlom, J. and Aaronson, S.A. (1984) Science 223, 364-370.
30. Saigo, K., Kugimiya, W., Matsuo, Y., Inouye, S., Yoskioka, K. and Yuki, S. (1984) Nature 312, 659-661.